

Behavior of Hybrid Double Skin Concrete Filled Circular Steel Tube Columns

Jin-Kook Kim¹, Hyo-Gyoung Kwak² and Ji-Hyun Kwak*²

¹Steel Structure Research Division, Research Institute of Industrial Science and Technology, Yeonsu, Incheon 406-840, Korea

²Civil and Environmental Engineering, Korea Advanced Institute of Science and Technology, Yuseong, Daejeon 305-701, Korea

(Received December 13, 2012, Revised January 15, 2013, Accepted February 05, 2013)

Abstract. A hybrid double skin concrete filled (HDSCF) circular steel tube column is proposed in this study. The yield strength of the outer steel tube is larger than 690MPa and the inner tube has less strength. In order to achieve efficiency with the high strength outer tube, a feasibility study on reducing the thickness of the tube below the specified design codes for CFTs was conducted based on an experimental approach. The experiment also took variables such as thickness of the inner tube, hollow ratio, and strength of concrete into consideration to investigate the behavior of the HDSCF column. In order to estimate the applicability of design equations for CFTs to the HDSCF column, test results from CFT and HDSCF columns with design codes were compared. It was found that the axial compressive performance of the proposed HDSCF column is equivalent to that of the conventional CFT member irrespective of design variables. Furthermore, the design equation for a circular CFT given by EC4 is applicable to estimate the ultimate strength of the HDSCF circular steel tube column.

Keywords: double skin; 690MPa; hybrid; CFT; confinement

1. Introduction

Concrete filled steel tubes (CFTs) were developed to enhance the strength, ductility, and energy absorption capacity of steel tubular members by confinement of core concrete filling the hollow tube and the use of a restraining steel tube against local buckling. Confinement in CFTs is continuous, unlike in the conventional spiral reinforced concrete columns. Therefore, CFTs are generally considered to possess favorable characteristics for use in regions of high seismic risk, and exhibit beneficial effects of composite behavior, where the concrete can carry stresses over the cylinder strength due to core confinement. Due to these advantages, CFTs are widely used in many buildings and bridges. Design specifications for CFTs have been well established (Eurocode (2004), AISC (2010), ACI (1999)) based on a number of experimental studies conducted by Gardner *et al.* (1967) and many others. Most of the studies were conducted using conventional steel of nominal yield strength not more than 460MPa, and specifications can be applied up to this level. Studies on higher strength steel are being conducted by a few researchers (Huang *et al.* 2002, Sakino *et al.*

*Corresponding author, Ph.D., E-mail: zethor@kaist.ac.kr

2004, Chung *et al.* 2010, Prakash *et al.* 2012), as structural steel with a nominal yield strength of 690MPa was developed several years ago. Researchers are also seeking to increase efficiency by using less steel.

A CFT is fully filled with concrete in its tubular section. This implies that concrete around the neutral axis, when bending moment is applied along with axial force, does not act as a structural element but rather as filler. The area around the neutral axis becomes large when the section is enlarged to increase the bending stiffness of the CFT. In order to improve the efficiency of the CFT, double skin (also known as a ‘sandwich tube’) composite sections, which have two steel tubes and an annulus between the tubes that is filled with concrete, has been studied by many researchers (Wei *et al.* 1995, Tao *et al.* 2004, Uenaka *et al.* 2010) since mid-1990s.

Early studies investigated whether the double skin provided performance advantages to CFTs such as strength increment by confinement of concrete, good local stability in steel tubes, and high ductility after the peak load under compression. Those works reported that concrete was well confined with a double skin tube and local buckling of the double skin steel tube was delayed, as in CFTs. Furthermore, the failure mode of the outer tube is local buckling, showing outward folding, similar to that in CFTs (Elchalakani *et al.* 2002, Zhao *et al.* 2002, Tao *et al.* 2004, Tao *et al.* 2006). However, these researches considered conventional steel grade lower than or equal to a yield strength of 460MPa at both the outer and inner tubes, and applied the same grade at both tubes. However, the inner tube does not require high strength, because it does not carry high stress when subjected to axial and bending loads. It plays an important role only in confinement of concrete between the tubes. Therefore, with the adoption of hybrid double skin steel tubes composed of a high strength outer steel tube and a low strength inner steel tube, additional economic and structural efficiency can be anticipated.

In this study, a hybrid double skin concrete filled (HDSCF) circular steel tube column is proposed. The yield strength of the outer steel tube is greater than 690MPa and the inner tube has less strength. In order to achieve efficiency with the high strength outer tube, a feasibility study on reducing the thickness of the tube below the level specified in design codes for CFTs was conducted based on an experimental approach. The experiment also took variables such as thickness of the inner tube, hollow ratio, and strength of concrete into consideration to investigate the behavior of the circular HDSCF column. In order to estimate the applicability of design guidelines for CFTs to the HDSCF column, test results from CFT and HDSCF columns with design equations were compared.

2. Design recommendations

2.1 AISC

The design rules for composite members in AISC (2010) follow the method for steel structures except for the evaluation of nominal strength and effective stiffness. Nominal strength of zero-length of a round filled composite member, P_{n0} , is classified according to the width-to-thickness ratio λ ($=D/t$) and given by

$$P_{n0} = A_s f_y + 0.95 A_c f_c \quad \lambda \leq \lambda_p \quad (1)$$

Eq. (1) Continued

$$P_{n0} = A_s f_y + 0.95 A_c f_c - \frac{0.25 A_c f_c}{(\lambda_r - \lambda_p)^2} (\lambda - \lambda_p)^2 \quad \lambda_p < \lambda \leq \lambda_r$$

$$P_{n0} = A_s \frac{0.72 f_y}{(\lambda f_y / E_s)^2} + 0.7 A_c f_c \quad \lambda_r < \lambda \leq \lambda_{\max}$$
(2)

where A_s and A_c are the area of steel and concrete, f_y is the yield strength of the steel tube, f_c is the strength of concrete, and E_s is the modulus of the steel tube. The limiting width-to-thickness ratios are $\lambda_p = 0.15E_s/f_y$, $\lambda_r = 0.19E_s/f_y$ and $\lambda_{\max} = 0.31E_s/f_y$. The compressive strength of the CFT, P_n , is determined for the limit state of flexural buckling based on member slenderness as follows

$$P_n = 0.658^{(P_{n0}/P_e)} P_{n0} \quad (3)$$

where P_e is the elastic critical buckling load determined by $\pi^2 EI_{eff}/(kL)^2$. The effective stiffness, EI_{eff} , for the composite member is $E_s I_s + (0.6 + 2A_s/(A_s + A_c)) E_c I_c$, where E_s and E_c are the modulus of the steel tube and concrete and I_s and I_c are the second moment of area of the steel tube and concrete, respectively. The above rule is applicable for a very short column up to $P_{n0}/P_e < 2.25$. All the test specimens manufactured in this study satisfy this condition. Limitation on the minimum yield strength for the steel tube is 525MPa and the minimum permitted thickness is $F_y D / 0.31E$ to prevent local buckling failure before yielding of steel.

2.2 Eurocode4 (EC4)

The plastic resistance to compression of a composite section in the Eurocode4 (2004) is given by

$$N_{pl,Rd} = A_s f_{yd} + 0.85 A_c f_{cd} \quad (4)$$

where f_{yd} and f_{cd} are the design values of the strength of the steel tube and concrete, respectively. For concrete filled sections, the coefficient of 0.85 may be replaced with a value of 1.0. In particular, for the circular CFT sections, the EC4 methodically considers the confinement effect. Due to the confinement effect, the strength of the concrete, tri-axially stressed, is increased by η_c while the strength of the steel tube, bi-axially stressed, is decreased by η_a . The plastic resistance of axial compression is given by

$$N_{pl,Rd} = \eta_a A_s f_{yd} + A_c f_{cd} \left(1 + \eta_c \frac{t}{D} \frac{f_y}{f_c} \right) \quad (5)$$

where f_c is the characteristic value of the strength of concrete, f_y is the nominal value of the yield strength of the steel tube, and t and D are the thickness and diameter of the steel tube, respectively. For comparison with experimental results, the exact measured values of strength of each material are used in this paper. On the other hand, application of design rules in EC4 is limited up to 460MPa regarding the nominal yield strength of structural steel. The steel contribution ratio δ

should be within the limits of 0.2 and 0.9, where δ is defined by $A_d f_{yd} / N_{pl,Rd}$. The minimum thickness of the steel tube to neglect the effects of local buckling is $f_y D / 21150$, which is a relatively conservative condition compared to the AISC.

3. Experimental investigation

3.1 Test specimens

23 specimens were designed for an ultimate load test. No.4 specimen, which complies with the minimum thickness rule of the EC4, was selected as the basic model. The thicknesses were designed to be 10mm and 2mm, and measured to be 9.53 and 2.0 for the outer tube and inner tube, respectively. The specimen uses 40MPa (f_c), 690MPa ($f_{y,out}$, yield strength), and 245MPa ($f_{y,in}$, yield strength) design strengths for the concrete, outer tube, and inner tube, respectively. Measured

Table 1 Geometry and material properties of test specimen

NO.	f_c (MPa)	$f_{y,out}$ (MPa)	$f_{y,in}$ (MPa)	$f_{c,m}$ (MPa)	$f_{y,out,m}$ (MPa)	$f_{y,in,m}$ (MPa)	D (mm)	H (mm)	t_{out} (mm)	t_{in} (mm)	R_h	A_c (mm ²)	$A_{s,out}$ (mm ²)	$A_{s,in}$ (mm ²)
1	40	-	-	40.8	-	-	300	600	-	-	0.5	53,014	-	-
2	40	690	-	59.9	765	-	300	600	9.53	-	0.5	44,318	8,696	-
3	40	-	245	59.9	-	311	300	600	-	2	0.5	52,059	-	955
4	40	690	245	56.6	765	311	300	600	9.53	2	0.5	43,363	8,696	955
5	40	690	245	56.6	765	311	300	600	9.53	2.3	0.5	43,217	8,696	1,100
6	40	690	245	56.6	765	302	300	600	9.53	3	0.5	42,876	8,696	1,442
7	40	690	245	56.2	765	311	300	600	9.53	2	0.7	26,021	8,696	1,332
8	40	690	245	56.9	765	311	300	600	9.53	2	0.7	26,021	8,696	1,332
9	40	690	245	56.9	765	311	300	600	9.53	2	0.7	26,021	8,696	1,332
10	40	690	245	59.9	765	311	300	600	9.53	2.3	0.7	25,819	8,696	1,534
11	40	690	245	59.9	765	302	300	600	9.53	3	0.7	25,346	8,696	2,007
12	40	690	245	56.9	765	311	300	600	4.78	2	0.5	47,626	4,433	955
13	40	690	245	56.6	765	311	300	600	4.78	2.3	0.5	47,481	4,433	1,100
14	40	690	245	59.9	765	311	300	600	4.78	2	0.7	30,284	4,433	1,332
15	40	690	245	59.2	765	311	300	600	4.78	2.3	0.7	30,083	4,433	1,534
16	40	690	245	56.9	765	311	300	600	7.72	2	0.5	44,971	7,089	955
17	40	690	245	56.9	765	311	300	600	7.72	2.3	0.5	44,825	7,089	1,100
18	27	690	245	35.7	765	311	300	600	9.53	2	0.7	26,021	8,696	1,332
19	27	690	245	38.5	765	311	300	600	9.53	2	0.7	26,021	8,696	1,332
20	27	690	245	38.5	765	311	300	600	9.53	2	0.7	26,021	8,696	1,332
21	50	690	245	64	765	311	300	600	9.53	2	0.7	26,021	8,696	1,332
22	50	690	245	65.1	765	311	300	600	9.53	2	0.7	26,021	8,696	1,332
23	50	690	245	65.3	765	311	300	600	9.53	2	0.7	26,021	8,696	1,332
CFT1	40	690	-	29	765	-	200	400	4.8	-	-	28,472	2,944	-
CFT2	40	690	-	29	765	-	200	400	4.8	-	-	28,472	2,944	-
CFT3	40	690	-	29	765	-	150	300	4.5	-	-	15,615	2,057	-
CFT4	40	690	-	29	765	-	150	300	4.5	-	-	15,615	2,057	-
CFT5	40	690	-	29	765	-	150	300	4.5	-	-	15,615	2,057	-

strengths were 56.6MPa ($f_{c,m}$), 765MPa (f_{y,out_m}), and 311MPa (f_{y,in_m}) for the concrete, outer tube, and inner tube. The hollow ratio (the ratio between the diameters of the outer tube and the inner tube, R_h) was chosen as 0.5, because a range of 0.4 to 0.6 is generally used in practice. The diameter (D) and height (H) of the specimens were determined to be 300mm and 600mm so as not to exceed the loading capacity of the test machine (UTM, universal test machine), which can apply load up to 10,000kN, and to avoid consideration of the slenderness effect. Other specimens were designed to investigate the ultimate strength with regard to variables such as (1) thickness of outer tube (t_{out} , 5mm, 8mm, 10mm), (2) thickness of inner tube (t_{in} , 2mm, 2.3mm, 3mm), (3) concrete cylinder strength (f_c , 27MPa, 40MPa, 50MPa), and (4) hollow ratio (R_h , 0.5, 0.7). Specimens No.1, which has no steel tube around the concrete, to No 3 were chosen to investigate the behavior of the specimens when they had no tube or only one of the two tubes. Details on the specimens can be found in Table 1 and pictures of the specimens are provided in Figure 1. For comparison with CFTs, five CFT columns with the same grade steel tube as the outer tube of the HDSCF column specimens were tested; two of them had 200mm diameter and the other three had 150mm diameter. Failure of the specimen was assumed to be when the load applied from the machine reached 85% of the maximum load after the peak point.

3.1.1 Effects of steel tubes

To investigate the behavior of the specimens when the internal or outer tubes are absent, hollow concrete specimens that have no steel tube (No.1), only an outer steel tube (No.2), only an inner tube (No.3), and both inner and outer encasing steel tubes (No.4~6) were tested. The measured ultimate strength, estimates from design rules, strength contributions of each material, and the ratios thereof are given in Table 2. The contribution of each material is calculated by simple multiplication of the area and measured strength of each material ($A_{sou} f_{y,out_m} + A_{s,in} f_{y,in_m}$ or $0.85A_c f_{c,m}$) and calculation of the contribution ratio follows the definition given in EC4.

The results of No.1 show that the measured strength is 67% of the calculated strength ($0.85A_c f_{c,m}$), thus indicating that the concrete column without reinforcement may be affected by hollowness and size because the aspect ratio of the specimen is the same as that of the cylinder for the concrete strength test. No. 3 shows a smaller ratio of measured strength to calculated strength than No. 1, and the strength difference between specimens No.1 and No.3 ($N_{exp,3} - N_{exp,1} = 1453\text{kN} - 1241\text{kN} = 212\text{kN}$) is less than the steel contribution ($N_{s,in} = A_{s,in} f_{y,in_m} = 297\text{kN}$). This shows that the contribution of the inner steel tube to the ultimate compressive strength is negligible, and a

Table 2 Test results: Effects of steel tubes (No.1~No.6)

NO.	N_{exp} (kN)	P_{n0} (kN)	P_n (kN)	$N_{pl,Rd}$ (kN)	N_{conc} (kN)	$N_{s,out}$ (kN)	$N_{s,in}$ (kN)	δ_o (%)	δ_{in} (%)	δ (%)	$\frac{N_{exp}}{P_n}$	$\frac{N_{exp}}{N_{pl,Rd}}$
1	1,241	1,839	1,829	1,839	1,839	-	-	-	-	-	0.68	0.67
2	9,512	8,909	8,895	8,909	2,256	6,653	-	71	-	71	1.04	0.79
3	1,453	2,948	2,934	2,948	2,651	-	297	-	10	10	0.50	0.49
4	10,000	9,281	9,267	11,960	2,332	6,653	297	71	3	74	1.08	0.84
5	10,000	9,319	9,304	11,973	2,324	6,653	342	70	4	74	1.07	0.84
6	10,000	9,394	9,379	11,994	2,305	6,653	435	70	5	74	1.07	0.83

δ_o : Outer steel contribution ratio given by $A_{s,out} f_{y,out_m} / N_{pl,Rd}$

δ_{in} : Inner steel contribution ratio given by $A_{s,in} f_{y,in_m} / N_{pl,Rd}$

δ : Total steel contribution ratio given by $\delta_o + \delta_{in}$

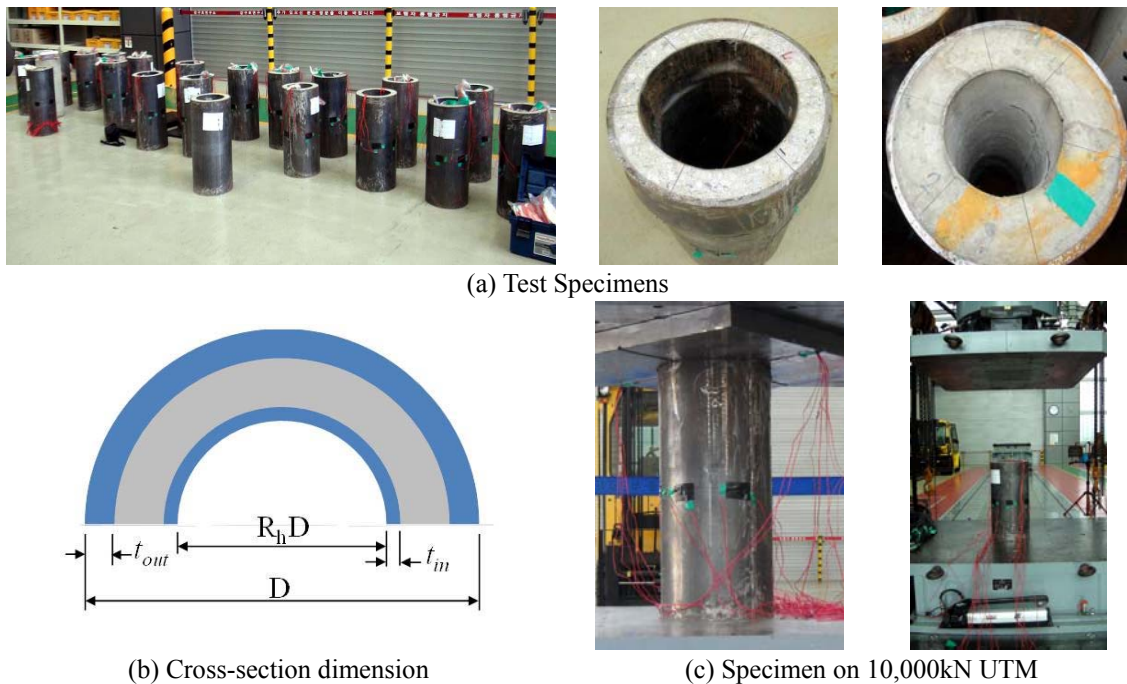


Fig. 1 Test specimens and experimental setup

confining effect for concrete is not expected when the outer steel tube is absent. The hollow concrete specimen (No.1) resists almost half of the cylinder strength only while specimen No.2, which is encased in an outer steel tube, exhibits ultimate strength exceeding simple summation of the strength contributions of the steel tube ($N_{s,out} = A_{s,out} f_{y,out,m}$) and concrete ($N_{conc} = 0.85A_c f_c$). Even though concrete is not entirely filled in specimen No.2, it seems that the outer steel tube confines the inner concrete to develop additional strength to some degree. Concrete is filled between two circular tubes in specimens No.4 to No.6. These specimens survived the test until the full capacity of the test machine. Therefore, the failure strengths are written as 10,000kN in Table 2. However, the exact ultimate strengths of these specimens are expected to exceed this value. The sole difference between specimens No.4~No.6 and No.2 is the existence of an inner steel tube. Nevertheless, the inner helps concrete to be entirely confined by preventing the expansion of concrete in the both the inner and outer directions when compressive load is applied up to failure. It can be concluded that the contribution of the inner steel tube is valuable when it is combined with an outer steel tube.

4. Performance of CFDST

To evaluate the compressive performance of a circular double skin tube (HDSCF) with respect to the design variables, specimens No.7~No.23 were investigated. Measured ultimate strength, estimates from design rules, strength contributions of each material, failure mode, and ductility parameters are given in Table 3. The displacement ductility μ is defined as the displacement at failure divided by the yield displacement (Kim *et al.* 2003).

4.1 Failure mode

Due to the manufacturing error of the tube and/or accidental eccentric loading of the test machine, bending moment may be delivered during the test. In such cases, local failure occurred with one-sided local buckling of the steel tube. The unexpected errors also led some specimens to fail near the top or bottom surfaces (see Fig. 2(a)). This may be attributed to stress concentration on the contacting area with the test machine. The failure shape of a well controlled test specimen shows symmetric ring-shaped local failure of the steel tube at the mid-height (see Fig. 2(b)). These two typical failure modes corresponding to the test results are described in Table 3. Repeated tests with specimens having the same geometry and material properties are performed with specimens Nos.7~9, Nos.18~20, and Nos.21~23. According to the load-displacement relations shown in Fig. 3, good repeatability on both ascending and descending curves is observed in Nos.7~9 while Nos.18~20 and Nos. 21~23 exhibit discrepancies on the softening branch. These differences may be explained by the failure modes. Specimens No.19, No.22, and No.23, which show eccentric failure, exhibit much lower ductility ratios than symmetrically failed specimens (Nos.18, No.20, and No.21).

Table 3 Test results: Effects of design variables (No.7~No.23 and CFT)

No	N_{exp} (kN)	P_n (kN)	$N_{pl,Rd}$ (kN)	N_{conc} (kN)	$N_{s,out}$ (kN)	$N_{s,in}$ (kN)	δ_o (%)	δ_{in} (%)	δ (%)	$\frac{N_{exp}}{P_n}$	$\frac{N_{exp}}{N_{pl,Rd}}$	Failure mode	μ
7	8,687	8,446	9,436	1,389	6,653	414	78	5	83	1.03	0.92	sym.	1.9
8	8,748	8,464	9,454	1,407	6,653	414	78	5	83	1.03	0.93	ecc.	1.6
9	8,546	8,464	9,454	1,407	6,653	414	78	5	83	1.01	0.90	ecc.	1.6
10	8,902	8,589	9,548	1,469	6,653	477	77	5	82	1.04	0.93	ecc.	1.5
11	8,684	8,691	9,577	1,442	6,653	606	76	7	83	1.00	0.91	sym.	2.2
12	8,118	5,424	7,843	2,574	3,391	297	53	5	58	1.50	1.04	sym.	1.4
13	7,268	5,452	7,849	2,553	3,391	342	53	5	58	1.33	0.93	ecc.	1.6
14	5,343	4,910	6,225	1,723	3,391	414	60	7	68	1.09	0.86	ecc.	1.2
15	5,735	4,947	6,232	1,692	3,391	477	60	8	68	1.16	0.92	sym.	1.4
16	8,619	8,040	10,455	2,431	5,423	297	66	4	69	1.07	0.82	ecc.	1.6
17	9,114	8,077	10,471	2,423	5,423	342	65	4	69	1.13	0.87	ecc.	1.8
18	8,360	7,940	8,911	883	6,653	414	83	5	88	1.05	0.94	sym.	2.2
19	8,656	8,009	8,982	952	6,653	414	82	5	88	1.08	0.96	ecc.	1.5
20	8,191	8,009	8,982	952	6,653	414	82	5	88	1.02	0.91	sym.	2.7
21	8,778	8,639	9,636	1,582	6,653	414	76	5	81	1.02	0.91	sym.	2.0
22	8,736	8,666	9,664	1,609	6,653	414	76	5	81	1.01	0.90	ecc.	1.6
23	8,364	8,671	9,670	1,614	6,653	414	76	5	81	0.96	0.86	ecc.	1.5
CFT1	4,086	3,032	4,631	784	2,252	-	73	-	73	1.35	0.88	-	-
CFT2	4,112	3,032	4,631	784	2,252	-	73	-	73	1.36	0.89	-	-
CFT3	3,925	2,001	3,081	430	1,574	-	78	-	78	1.96	1.27	-	-
CFT4	3,899	2,001	3,081	430	1,574	-	78	-	78	1.95	1.27	-	-
CFT5	3,577	2,001	3,081	430	1,574	-	78	-	78	1.79	1.16	-	-

sym.: symmetric local buckling

ecc.: eccentric local buckling near the top or bottom surface



(a) Failure near the top surface (No.19)

(b) Symmetric buckling in the mid-height(No.20)

Fig. 2 Failure modes

Strain gages attached to the steel tube indicate that the steel tube yielded before the peak load. However, local buckling occurred in the softening region in the load-displacement relation regardless of whether depth to thickness ratio limit of the outer steel tube satisfies the EC4 condition. This implies that the depth to thickness ratio has no impact on the ultimate strength in these specimens. Pictures of typical specimens that satisfy the EC4 D/t ratio (No.10) and do not satisfy it (No.15) after the loading test are shown in Fig. 4. Notable differences in the failure mode of two typical specimens are not found.

4.2. Effects of design parameters on ultimate strength

Effects of the D/t ratio of the outer steel tube, hollow ratio, strength of concrete, and steel contribution ratio to the ultimate resisting capacity of the circular HSCDF column are investigated. Measured ultimate strengths are presented in Figure 5 as ratios to estimates from design equations (AISC: Eqn.(2) and EC4: Eqn.(4)) to evaluate the applicability of existing design guidelines for a circular CFT column. To this end, the measured strength, instead of the design strength, of each material is adopted to calculate the ultimate resisting capacity from the design equations. The definition of the steel contribution ratio in Figure 5(e) is given in EC4 and also shown in Table 2.

The design equation for the circular CFT from EC4 gives a consistent estimation of the ultimate strength of the circular HDSCF specimens without showing any trend regarding the design variables such as the depth to thickness ratio, thickness of the inner tube, strength of concrete, hollow ratio, and steel contribution ratio. Ratios between the measured and calculated range from 0.82 to 1.04. This indicates that the design equation of EC4 for the CFT column can be used for estimation of the ultimate strength of the HDSCF column with or without some calibration, even though the column does not meet the requirements of the D/t ratio and the yield strength of the outer steel tube. In contrast to EC4, the AISC design equation tends to underestimate the ultimate strength, especially when the D/t ratio is higher, and the hollow ratio and steel contribution ratios are lower while dependencies on the strength of concrete and the thickness of the inner steel tube are not

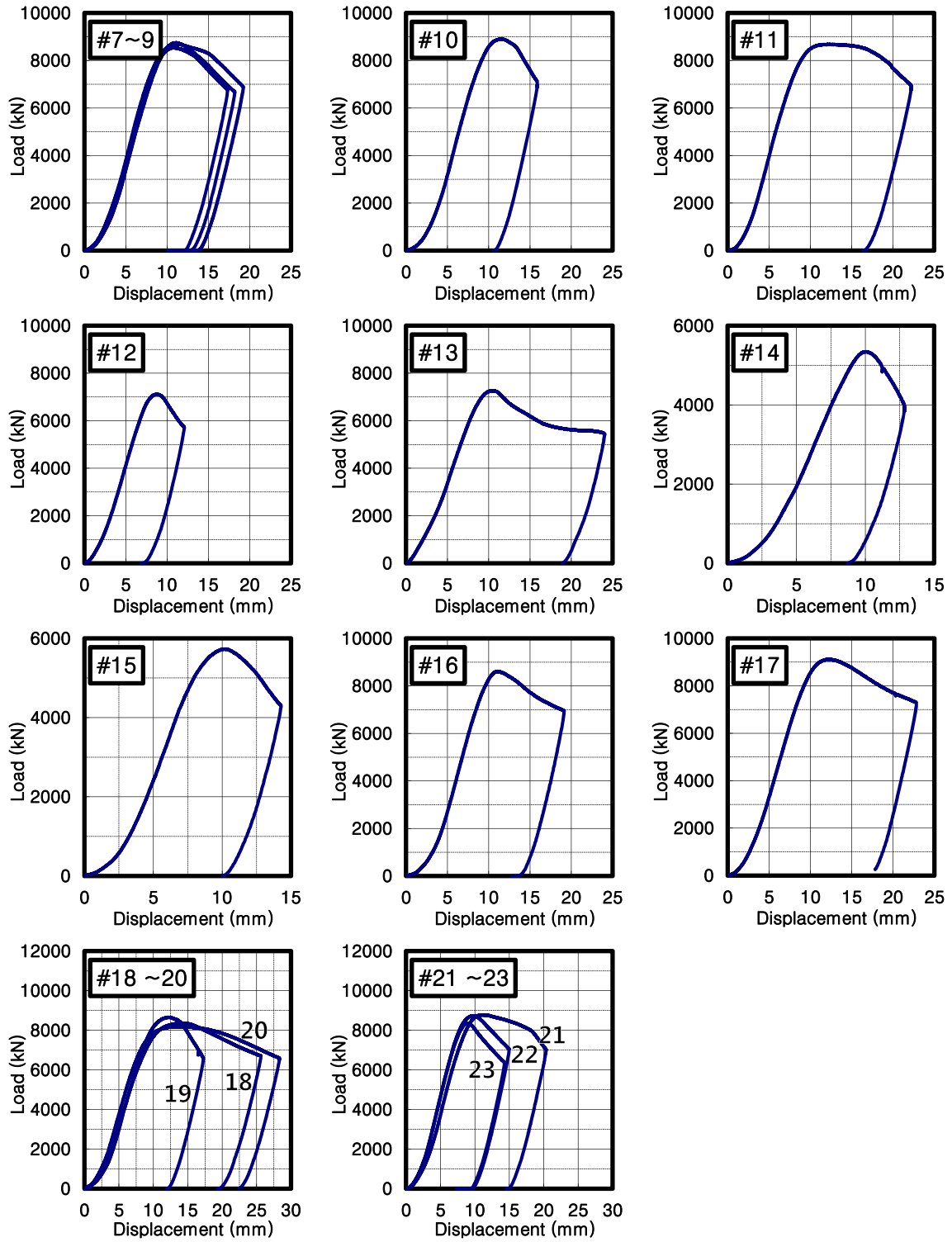


Fig. 3 Load-displacement relations of HDSCF

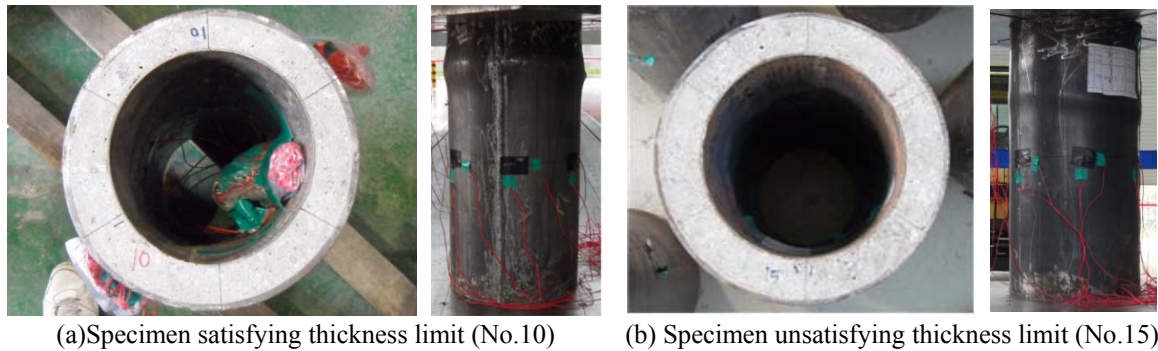


Fig. 4 Shape of specimens after failure

found. In addition, the AISC design equation generally gives a conservative estimation compared to the EC4. It appears that the confinement effect of concrete is not sufficiently considered in the AISC code. On the contrary, estimates from EC4 tend to overestimate the ultimate strength of the specimens, even though they are consistent. This is due to the calculation of ultimate resisting capacity being based on the measured strength of materials instead of the design strength.

A total of 109 test results of circular CFT (9 tests from Gardner *et al.* (1967); 3 tests from Yamamoto *et al.* (2002); 16 tests from Sakino *et al.* (2004); 8 tests from Yu *et al.* (2007); 12 tests from Han *et al.* (2005); 2 tests from Schneider (1998); 3 tests from Huang *et al.* (2002); 6 tests from Tomii *et al.* (1977); 6 tests from Hwang *et al.* (2003); 10 tests from O'shea *et al.* (2000); 5 tests from this study named 'CFT' in the figure) and HDSCF columns (12 tests from Tao *et al.* (2004); 17 tests from this study named 'HDSCF' in the figure) are plotted in Figure 6. In this figure, the y-axis represents the measured ultimate strength of each test result divided by the corresponding design strength calculated using the EC4 equation, and the x-axis represents the yield strength of the outer steel tube. The figure shows that most of the test results range from 0.8 to 1.0 including those in this study with no respect to the yield strength of the steel tube. Therefore, it can be concluded that the EC4 design equation can give a reasonable strength estimation for the HDSCF column using 690MPa nominal yield strength at the outer steel tube and half the thickness of the steel tube specified in the design code.

4.3. Effects of design parameters on softening

Even though this study deals with a column subject to only compression force without bending moment, softening behaviors were reviewed according to design variables, because the softening characteristics are highly related to the ductility of a column under seismic loading. Softening behavior of test specimens can be observed through load versus displacement curves illustrated in Fig. 3. This figure shows that all the ascending curves are similar but the descending parts are different. This reveals that the design variables affect not only the ultimate strength but also the softening behavior. In order to quantify the softening behavior, the same concept as the ductility of the column was adopted (Kim *et al.* 2003) and ductility parameters obtained from the load-displacement relation are given in Table 3. The displacement ductility is plotted in Fig. 7 against the thickness of the inner and outer steel tubes. Numbers in the legend represent the thickness of the outer steel tube and the hollow ratio, respectively. The most ductile specimen is No.11, which

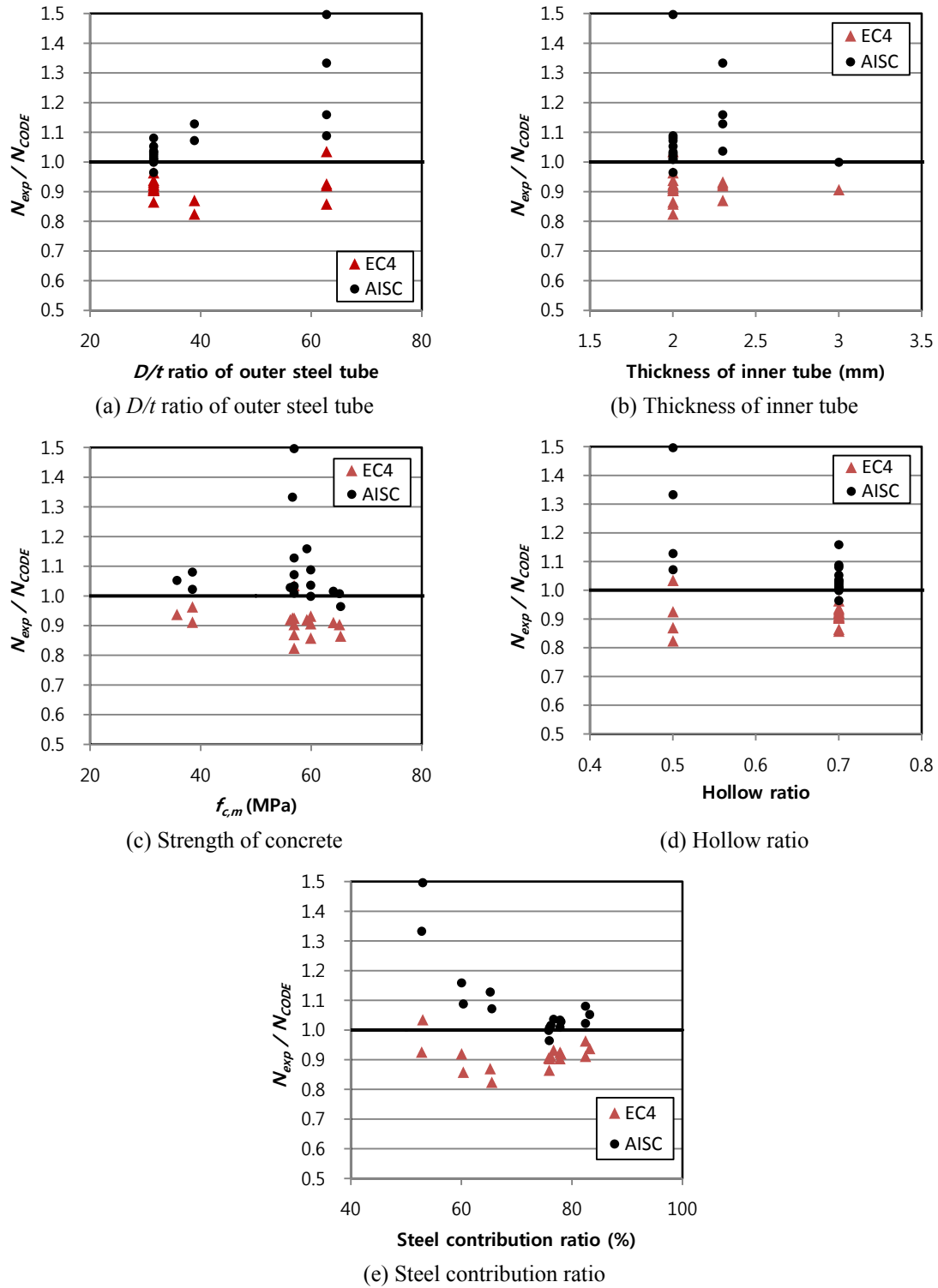


Fig. 5 Ratios between design rules and measured strength in accordance with design variables

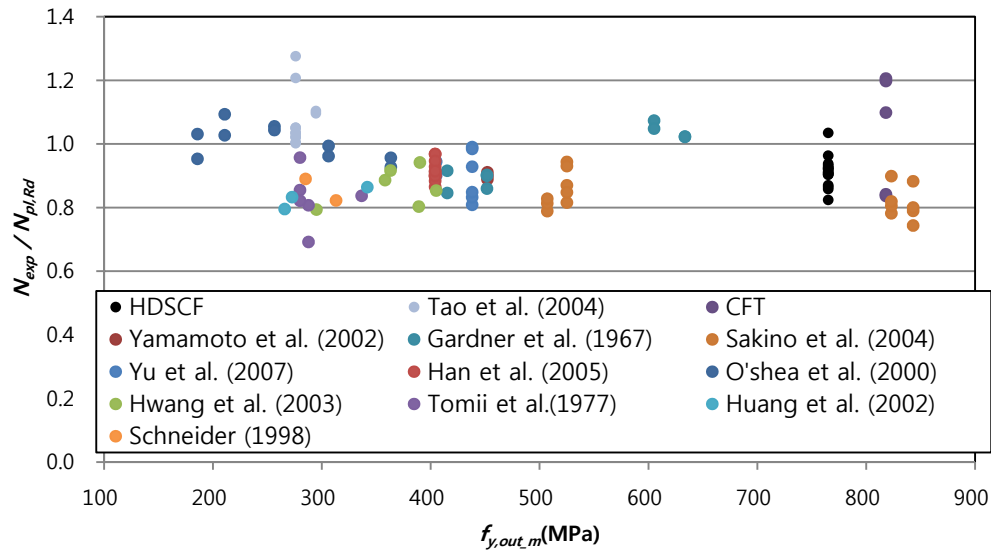


Fig. 6 Ratios between $N_{pl,Rd}$ and N_{exp} against yield strength of outer steel tube

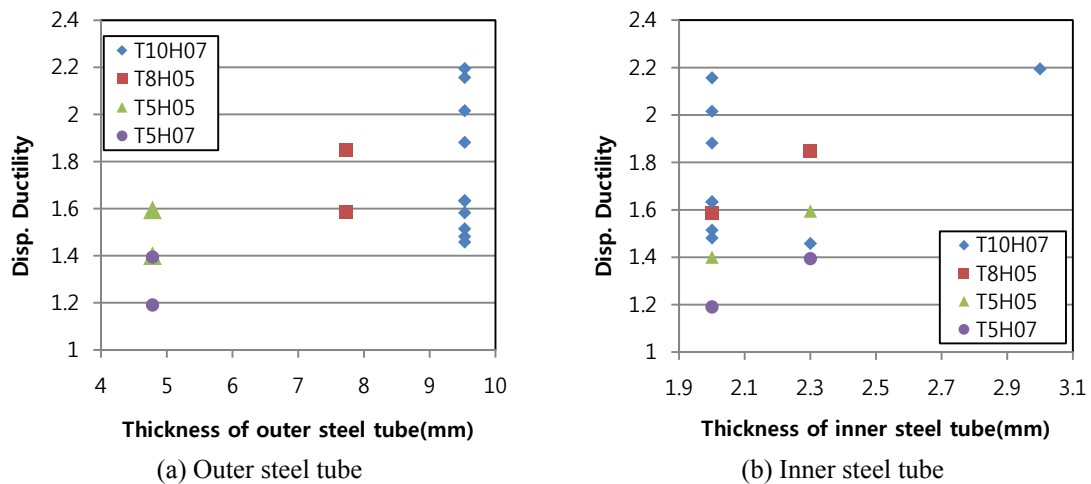


Fig. 7 Displacement ductility in accordance with thickness of steel tube

uses a 10 mm thick outer tube with a 3 mm thick inner tube. The results shown in Fig. 7(a) indicate that the displacement ductility almost linearly increases as the thickness of the outer steel tube increases in an average manner. This trend is the same as that observed by other researchers (Han 2000, Tao *et al.* 2004). The effect of thickness of the inner steel tube on the displacement ductility is not clear when the outer steel tube is 10mm thick (see diamond dots in Fig. 7(b)). But it was observed from the same figure that specimens with a 2.3mm thick inner steel tube exhibit more ductile behavior than those with a 2mm thick inner steel tube when the thickness of the outer steel tube is less than 10mm. Therefore, use of a thin, high strength outer tube and a relatively thick, low strength inner tube can be a good option for enhancing the efficiency of the HDSCF column.

5. Conclusions

In this paper, axial compressive experiments on a hybrid double skin concrete filled (HDSCF) circular steel tube column using a high strength outer steel tube ($f_{y,out} = 690$ MPa) and a low strength inner steel tube ($f_{y,in} = 245$ MPa) were conducted. The effects of design variables on the compressive behavior of the specimens were analyzed. Furthermore, a comparison of test results from CFT and HDSCF columns with design codes was made in order to estimate the applicability of design equations for CFT to HDSCF columns. From the test results, the following conclusions were obtained:

- (1) HDSCF circular column exhibited consistent compressive performance irrespective of the hollow ratio, strength of concrete, and thickness of the outer steel tube.
- (2) For specimens with a thinner outer steel tube (No.12~No.17), local buckling did not occur before their ultimate strength was developed. Therefore, D/t limitation in EC4 should be mitigated to 50%.
- (3) The conventional design equation for a circular CFT column given in EC4 is applicable to the HDSCF circular steel tube column while the design equation given in AISC gives conservative estimation.
- (4) Ductility of the HDSCF column is proportional to the thickness of the outer steel tube and can be assisted by a thicker inner steel tube when the outer steel tube is relatively thinner than the design rule.
- (5) Use of a HDSCF column with a thin, high strength outer tube and a relatively thick, low strength inner tube can be a good option for efficient design.

Acknowledgment

This research was supported by a grant from the Construction Technology Innovation Program(09CTIPE04) funded by Ministry of Land, Transportation and Maritime Affairs(MLTM) of Korean government and financially supported by Korea Minister of Ministry of Land, Transport and Maritime Affairs(MLTM) as 'U-City Master and Doctor Course Grant Program.

References

- ACI (1999), Building code requirements for reinforced concrete (ACI 318-99), American Concrete Institute, Detroit.
- AISC (2010), Specification for structural steel buildings, American Institute of Steel Construction, Chicago, IL.
- Chung, K.S., Lee, S.J., Ryu, J.H. and Kim, J.H. (2010), "Prediction of the structural behavior of high strength concrete-filled square steel tube column subjected to flexural and eccentric loading", *Architectural Res.*, **26**(15), 115-123.
- Elchalakani, M., Zhao, X. and Grzebieta, R. (2002), "Plastic mechanism analysis of circular tubes under pure bending", *Int. J. of Mechanical Sci.*, **44**(6), 1117-1143.
- Eurocode4 (2004), Design of composite steel and concrete structures part 2, General rules and rules for bridges, Brussels.
- Gardner, N.J. and Jacobson, E.R. (1967), "Structural behavior of concrete filled steel tubes", *ACI Journal*, **64**(7), 404-412.

- Han, L.H. (2000), Concrete filled steel tubular structures, China Science Press, Beijing.
- Han, L.H., Yao, G.H. and Zhao, X.L. (2005), "Tests and calculations for hollow structural steel (HSS) stub columns filled with self-consolidating concrete (SCC)", *J. of Constr. Steel Res.*, **61**(9), 1241-1269.
- Huang, C.S., Yeh, Y.K., Liu, G.Y., Hu, H.T., Tsai, K., Weng, Y., Wang, S. and Wu, M.H. (2002), "Axial load behavior of stiffened concrete-filled steel columns", *J. of Struct. Eng.*, **128**(9), 1222-1230.
- Hwang, W.S., Kim, D.J. and Jung, D.A. (2003), "Ultimate strength of CFT short columns considering the confining effect of concrete", *KSCE Journal*, **23**(5), 807-1064.
- Kim, T.H., Lee, K.M., Yoon, C. and Shin, H.M. (2003), "Inelastic behavior and ductility capacity of reinforced concrete bridge piers under earthquake. II: Numerical validation", *J. of Struct. Eng.*, **129**(9), 1208-1219.
- O'Shea, M.D. and Bridge, R.Q. (2000), "Design of circular thin-walled concrete filled steel tubes", *J. of Struct. Eng.*, **126**(11), 1295-1303.
- Prakash, A., Anandavalli, N., Madheswaran, C.K. and Lakshmanan, N. (2012), "Experimental investigation on flexural behaviour of HSS stud connected steel-concrete composite girders", *Steel. Compos. Struct.*, **13**(3), 239-258.
- Sakino, K., Nakahara, H., Morino, S. and Nishiyama, I. (2004), "Behavior of centrally loaded concrete-filled steel-tube short columns", *J. of Struct. Eng.*, **130**(2), 180-188.
- Schneider, S.P. (1998), "Axially loaded concrete-filled steel tubes", *J. of Struct. Eng.*, **124**(10), 1125-1138.
- Tao, Z. and Han, L.H. (2006), "Behaviour of concrete-filled double skin rectangular steel tubular beam-columns", *J. of Constr. Steel Res.*, **62**(7), 631-646.
- Tao, Z., Han, L.H. and Zhao, X.L. (2004), "Behaviour of concrete-filled double skin (CHS inner and CHS outer) steel tubular stub columns and beam-columns", *J. of Constr. Steel Res.*, **60**(8), 1129-1158.
- Tomii, M., Yoshimura, K. and Morishita, Y. (1977), "Experimental studies on concrete filled steel tubular stub columns under concentric loading", *International Colloquium on Stability of Structures under Static and Dynamic Loads*, Washington, D.C.
- Uenaka, K., Kitoh, H. and Sonoda, K. (2010), "Concrete filled double skin circular stub columns under compression", *Thin-Walled Struct.*, **48**(1), 19-24.
- Wei, S., Mau, S., Vipulanandan, C. and Mantrala, S. (1995), "Performance of new sandwich tube under axial loading: experiment", *J. of Struct. Eng.*, **121**(12), 1806-1814.
- Yamamoto, T., Kawaguchi, J. and Morino, S. (2002), "Experimental study of the size effect on the behavior of concrete filled circular steel tube columns under axial compression", *J. Struct. Constr. Eng.*, (561), 237-244.
- Yu, Z., Ding, F. and Cai, C. (2007), "Experimental behavior of circular concrete-filled steel tube stub columns", *J. of Constr. Steel Res.*, **63**(2), 165-174.
- Zhao, X.L., Han, B. and Grzebieta, R.H. (2002), "Plastic mechanism analysis of concrete-filled double-skin (SHS inner and SHS outer) stub columns", *Thin-Walled Struct.*, **40**(10), 815-833.